doi:10.1093/brain/awp233 Brain 2010: 133; 286–299 | 286

BRAIN
A JOURNAL OF NEUROLOGY

Language networks in semantic dementia

Federica Agosta,[1,2] Roland G. Henry,[3] Raffaella Migliaccio,[1,4] John Neuhaus,[5] Bruce L. Miller,[1] Nina F. Dronkers,[6,7] Simona M. Brambati,[1,8] Massimo Filippi,[2] Jennifer M. Ogar,[1] Stephen M. Wilson[1] and Maria Luisa Gorno-Tempini[1,9]

1 Memory and Aging Center, Department of Neurology, University of California, San Francisco, CA, USA
2 Neuroimaging Research Unit, Institute of Experimental Neurology, Scientific Institute and University Hospital San Raffaele, Milan, Italy
3 Department of Radiology and Biomedical Imaging, University of California, San Francisco, CA, USA
4 Department of Neurological Sciences, II University of Naples, Naples, Italy
5 Department of Epidemiology and Biostatistics, University of California, San Francisco, CA, USA
6 Center for Aphasia and Related Disorders, VA Northern California Health Care System, Martinez, CA, USA
7 Department of Neurology, University of California, Davis, CA, USA
8 Centre de recherche, Institut Universitaire de Gériatrie de Montréal, Montréal, Québec, Canada
9 Center for Mind/Brain Sciences (CIMeC), University of Trento, Trento, Italy

Correspondence to: Maria Luisa Gorno-Tempini,
Memory and Aging Center,
Department of Neurology,
University of California,
San Francisco, 350 Parnassus Avenue,
Suite 905, San Francisco,
CA 94143-1207, USA
E-mail: marilu@memory.ucsf.edu

Cognitive deficits in semantic dementia have been attributed to anterior temporal lobe grey matter damage; however, key aspects of the syndrome could be due to altered anatomical connectivity between language pathways involving the temporal lobe. The aim of this study was to investigate the left language-related cerebral pathways in semantic dementia using diffusion tensor imaging-based tractography and to combine the findings with cortical anatomical and functional magnetic resonance imaging data obtained during a reading activation task. The left inferior longitudinal fasciculus, arcuate fasciculus and fronto-parietal superior longitudinal fasciculus were tracked in five semantic dementia patients and eight healthy controls. The left uncinate fasciculus and the genu and splenium of the corpus callosum were also obtained for comparison with previous studies. From each tract, mean diffusivity, fractional anisotropy, as well as parallel and transverse diffusivities were obtained. Diffusion tensor imaging results were related to grey and white matter atrophy volume assessed by voxel-based morphometry and functional magnetic resonance imaging activations during a reading task. Semantic dementia patients had significantly higher mean diffusivity, parallel and transverse in the inferior longitudinal fasciculus. The arcuate and uncinate fasciculi demonstrated significantly higher mean diffusivity, parallel and transverse and significantly lower fractional anisotropy. The fronto-parietal superior longitudinal fasciculus was relatively spared, with a significant difference observed for transverse diffusivity and fractional anisotropy, only. In the corpus callosum, the genu showed lower fractional anisotropy compared with controls, while no difference was found in the splenium. The left parietal cortex did not show significant volume changes on voxel-based morphometry and demonstrated normal functional magnetic resonance imaging activation in response to reading items that stress sublexical phonological processing. This study shows that semantic dementia is associated with anatomical damage to the major superior and inferior temporal white matter connections of the left hemisphere likely involved in semantic and lexical processes, with relative sparing of the fronto-parietal superior longitudinal fasciculus. Fronto-parietal regions connected by this tract were activated normally in the same patients during sublexical reading. These findings contribute to our understanding of the anatomical changes that occur in semantic dementia, and may further help to explain the dissociation between marked single-word and object knowledge deficits, but sparing of phonology and fluency in semantic dementia.

Received July 20, 2009. Accepted July 26, 2009. Advance Access publication September 16, 2009

Keywords: semantic dementia; semantic knowledge; diffusion tensor-based tractography; functional MRI; voxel-based morphometry

Abbreviations: ATL = anterior temporal lobe; BA = Brodmann area; DTI = diffusion tensor imaging; FA = fractional anisotropy; FACT = fibre-assignment-by-continuous-tracking; fMRI = functional magnetic resonance imaging; ILF = inferior longitudinal fasciculus; $\lambda_{//}$ = parallel diffusivity; $\lambda_{\perp}$ = transverse diffusivity; MD = mean diffusivity; ROI = region of interest; SLF = superior longitudinal fasciculus

Introduction

Semantic dementia is a clinical variant of primary progressive aphasia and it is associated with progressive deterioration of semantic knowledge, atrophy of the anterior temporal lobe (ATL) and most often TAR DNA binding protein-43 related pathology (Hodges *et al*., 1992; Snowden *et al*., 1992; Mummery *et al*., 2000; Rosen *et al*., 2002; Davies *et al*., 2005). The pattern of impairment in semantic dementia is characterized by a clear dissociation between marked single-word comprehension, object knowledge and irregular word reading deficits, and sparing of fluency, phonology, syntax and working memory (Patterson and Hodges, 1992; Hodges and Patterson, 1996; Gorno-Tempini *et al*., 2004).

Semantic deficits in semantic dementia have been attributed to grey matter damage to the ATL (Mummery *et al*., 2000; Galton *et al*., 2001; Rosen *et al*., 2002; Gorno-Tempini *et al*., 2004), but the language network is a highly interactive system and the role of altered anatomical and functional connectivity must be considered. Results from several functional neuroimaging studies conducted in semantic dementia suggest that certain aspects of the syndrome could be due to a disconnection between the ATL and other spared language areas (Mummery *et al*., 1999; Sonty *et al*., 2007; Wilson *et al*., 2009). For instance, the ATL disconnection could cause a dysfunction in the activity of posterior temporal regions, i.e. 'functional diaschisis' (Mummery *et al*., 1999), altered functional connectivity between Wernicke's and Broca's areas (Sonty *et al*., 2007) or even compensatory hyperactivation in the inferior parietal area (Sonty *et al*., 2007; Wilson *et al*., 2009). Structural connectivity also needs to be investigated, but evidence regarding the integrity of language white matter tracts in semantic dementia and related disorders is still lacking.

Anatomical, network-level structural connectivity can be investigated with diffusion tensor imaging (DTI)-based tractography that allows *in vivo* segmentation of axonal trajectories, by measuring the diffusivity of water along different directions on a voxel-by-voxel basis (Conturo *et al*., 1999; Basser *et al*., 2000; Wakana *et al*., 2004; Catani and Thiebaut de Schotten, 2008). Once the tract is identified, values of fibre integrity can be obtained including fractional anisotropy (FA), a measure of the degree to which water diffusion has a common orientation, and mean diffusivity (MD), a measure of the magnitude of water diffusion (Basser *et al*., 1994). Furthermore, analysis of directional diffusivities—parallel ($\lambda_{//}$) and transverse ($\lambda_{\perp}$)—may provide additional information on the underlying mechanisms of white matter integrity loss (Basser *et al*., 1994). Myelin breakdown is consistently associated with increased diffusivity perpendicular to the white matter tract ($\lambda_{\perp}$), while axonal damage is reflected in diffusivity changes parallel ($\lambda_{//}$) to the primary fibre orientation (Beaulieu, 2002; Song *et al*., 2002; Sullivan *et al*., 2008; Vernooij *et al*., 2008). DTI metrics are sensitive to the pathology of a number of neurological conditions that result in axonal loss and/or disruption of myelin sheath, such as stroke, multiple sclerosis, brain tumours and dementia (Rovaris *et al*., 2005; Ciccarelli *et al*., 2008). To our knowledge, the only previous DTI-based tractography study that included semantic dementia patients in a group analysis identified DTI changes in the corpus callosum and principal association fibres [i.e. uncinate fasciculus, inferior longitudinal fasciculus (ILF) and arcuate fasciculus] (Matsuo *et al*., 2008), however, the few semantic dementia patients were not the focus of the study but were incorporated into a larger cohort of behavioural frontotemporal dementia subjects, and the contribution of semantic dementia patients to the overall finding is uncertain (Matsuo *et al*., 2008).

The main white matter tracts that have been involved in language processing are the ILF, the superior longitudinal fasciculus (SLF), and the arcuate (Lu *et al*., 2002; Mandonnet *et al*., 2007; Catani and Mesulam, 2008; Duffau, 2008; Glasser and Rilling, 2008). The ILF is a ventral associative bundle which connects the temporal and occipital lobes, running along the lateral walls of the inferior and posterior horns of the lateral ventricle (Catani *et al*., 2003; Catani and Thiebaut de Schotten, 2008). The SLF is a long associative bundle connecting the frontal regions with parieto-temporal areas. It can be subdivided into different components (Petrides and Pandya, 1984; Makris *et al*., 2005; Schmahmann *et al*., 2007). Of interest to our study, subcomponent II (SLF II) links the inferior parietal lobule with the posterior and caudal prefrontal cortex, whereas SLF III connects the rostral inferior parietal lobule with the ventral part of premotor and prefrontal cortex (Petrides and Pandya, 1984; Makris *et al*., 2005; Schmahmann *et al*., 2007). Another fibre tract within the SLF, the arcuate fasciculus, connects the caudal part of the superior and middle temporal gyri to the lateral prefrontal cortex (Petrides and Pandya, 1984; Makris *et al*., 2005; Schmahmann *et al*., 2007). To our knowledge, the integrity of these white matter tracts in the semantic dementia and its relation to structural and functional status of the cortex have never been investigated.

In this study, we used a multimodal imaging approach to study the integrity of the left-hemisphere language network in semantic dementia patients and healthy controls. In particular, we investigated DTI-based macro- and micro-anatomical changes in the left ILF, arcuate fasciculus and fronto-parietal SLF. The left uncinate fasciculus and the genu and splenium of the corpus callosum were also obtained for comparison with previous studies in frontotemporal dementia (Matsuo *et al*., 2008; Zhang *et al*., 2009). Patients and controls underwent grey matter structural and functional magnetic resonance imaging (fMRI) studies, allowing us to investigate the relationship between white matter findings and grey matter integrity and functionality. We hypothesized that semantic dementia would be associated with: (i) anatomical damage to a

ventral pathway including the ILF and ATL structures, and with altered activation in lateral and ventral grey matter structures; and (ii) relative sparing of the dorsal fronto-parietal language pathway.

Materials and methods

Subjects

Five patients with semantic dementia were recruited at the Memory and Ageing Centre, University of California, San Francisco (UCSF). The diagnosis of semantic dementia was based on published criteria (Hodges *et al*., 1992; Neary *et al*., 1998) determined by a multidisciplinary evaluation, including neurological history and examination, caregiver interview, and neuropsychological testing of memory, executive functions, visuospatial skills, language and mood. During the diagnostic work-up, neuroimaging findings were used only to exclude other causes of focal or diffuse brain damage, including extensive white matter disease. In order to be able to perform the reading fMRI task (Wilson *et al*., 2009), patients were required to score at least 15 out of 30 on the Mini Mental Status Exam (MMSE), be fluent in English and be able to tolerate the long MRI study. Nine semantic dementia patients met these criteria and were considered for this study. Among these, two patients were not scanned (one was unable to be scheduled, and the other was judged too behaviourally impaired to undergo MRI), and data were unusable for other two due to technical problems. Thus, imaging data were successfully acquired and analysed for five semantic dementia cases. Demographic information and neuropsychological data for these patients are shown in Table 1. Nine healthy age-matched control subjects also underwent fMRI (Wilson *et al*., 2009) and DTI scanning, but one DTI scan was not analysed because of poor quality. Control subjects had to have a normal neurological exam, neuropsychological testing and MRI.

Voxel-based morphometry (Ashburner and Friston, 2005) was used to investigate patterns of grey matter and white matter atrophy in the five semantic dementia patients relative to a larger control group of 48 age- and sex-matched healthy subjects [38 females, 10 males; mean age 61.5 years; standard deviation (SD) 10.3].

All participants gave written informed consent, and the study was approved by the Committee on Human Research at UCSF.

Cognitive testing

Each subject participated in a neuropsychological screening battery testing for language, executive and visuospatial functioning, and visual–non-verbal and verbal episodic memory, as described earlier (Kramer *et al*., 2003). Semantic dementia patients also underwent a comprehensive speech and language evaluation, as previously reported (Gorno-Tempini *et al*., 2004). Demographic, clinical and neuropsychological differences between groups were analysed using independent sample *t*- and χ^2-tests as appropriate.

MRI acquisition

Structural, DT and fMRIs were acquired on a 3 Tesla GE Signa EXCITE MRI system (General Electric, Waukesha, WI) at the UCSF Department of Radiology. An eight-channel head coil with array spatial sensitivity encoding technique (ASSET) parallel imaging factor of 2 was used to acquire single-shot spin-echo echo-planar images with axial slices covering the whole brain: 50 interleaved slices with 2.2 mm thickness; repetition time (TR)/echo time (TE) = 6200 ms/74 ms; flip angle = 90°; field of view (FOV) = 280 mm^2; matrix = 128 × 128; voxel size = 2.2 × 2.2 × 2.2 mm^3; number of acquisition (NEX) = 1; 5/8 partial Fourier encoding. Diffusion gradients were applied in 55 directions uniformly distributed on a sphere through electrostatic repulsion with $b = 2000$ s/mm^2. Peak gradient strength was 40 mT/m. An image set with minimal diffusion weighting (NEX = 4) and a T_2-weighted fast-spin echo volume (TR/TE = 3550/74.6 ms; matrix = 256 × 256; 2.2 mm slice thickness; 280 mm^2 FOV), in the same plane as the DTI data, were also obtained. Functional T_2*-weighted images were acquired with the following parameters: two runs of 232 volumes each; 23 axial slices with 4 mm thickness and 1 mm gap; TR/TE = 1650/30 ms; FOV = 220 mm^2; matrix 64 × 64; voxel size 3.4 × 3.4 × 5 mm^3. High-resolution T_1-weighted spoiled gradient echo (180 contiguous axial slices with 1-mm thickness; TR/TE = 7 ms/1.65 ms; inversion time = 400 ms; flip angle = 15°; FOV = 256 mm^2; matrix = 256 × 256; voxel size 1.0 × 1.0 × 1.0 mm^3; NEX = 1) and T_2-weighted fast spin echo (FSE) (23 axial slices with 4-mm thickness and 1-mm gap; TR/TE = 4850 ms/74.7 ms; flip angle = 90°; echo train length = 16; FOV = 256 mm^2; matrix = 192 × 256; voxel size = 1.0 × 1.0 × 5.0 mm; NEX = 1) sequences were also acquired.

T_1-weighted structural images for voxel-based morphometry analysis were collected for the five semantic dementia patients and 48 matched healthy controls as part of the screening evaluation at the UCSF Memory and Aging Centre. These images were acquired on a 1.5 Tesla Siemens Magnetom VISION system (Siemens, Iselin, NJ) equipped with a standard quadrature head coil. A volumetric magnetization prepared rapid gradient echo sequence of the whole brain was acquired (164 contiguous coronal slices with 1.5-mm thickness; TR/TE = 10 ms/4 ms; flip angle = 15°; FOV = 256 mm^2; matrix = 256 × 256; voxel size = 1.0 × 1.0 × 1.5 mm^3).

DTI analysis

DT images were transferred off-line, and diagonalization of the images (Basser *et al*., 1994) was performed using an in-house software written in the C language. Directional diffusivities were defined as $\lambda_{//}$ being the largest eigenvalue, and $\lambda_{\perp}$ being the average of the minor eigenvalues. We calculated the directionally averaged diffusion or MD as the mean of all three eigenvalues, and FA from the diffusion eigenvalues (Basser *et al*., 1994).

Fibre tracking

Fibre tracking was performed using an in-house software written in Interactive Data Language (IDL; ITT Visual Information Solutions, Boulder, CO) (Berman *et al*., 2005) based on the Fibre-Assignment-by-Continuous-Tracking method (FACT) (Mori *et al*., 1999). The fibre-tracking software allows identification of fibre tracts, visualization in 3D, and quantitative analyses on the delineated tracts. Fibre tracts were launched from every voxel in the brain. This approach reduces biases inherent to the use of local starting points (Mori *et al*., 1999). Fibre trajectories follow the primary eigenvector from voxel to voxel in 3D. Fibre tracts were terminated upon entering a voxel if the FA value was less than 0.15, or voxel-to-voxel deflection angle was >50°. Using FACT, tracking the major brain fibre bundles is reported to be highly reproducible (Mori *et al*., 1999; Wakana *et al*., 2004).

The trajectories of the ILF, the arcuate fasciculus, the fronto-parietal SLF, and the uncinate fasciculus in the left hemisphere, as well as of the genu and splenium of the corpus callosum were obtained. By cross-referencing neuroanatomical (Dejerine, 1895) and previous tractography works (Catani *et al*., 2002; Makris *et al*., 2005; Catani and Thiebaut de Schotten, 2008; Glasser and Rilling, 2008), regions of

Table 1 Demographic, clinical and cognitive assessment information on each semantic dementia patient and healthy control participants

	Case 1	Case 2	Case 3	Case 4	Case 5	Controls ($n = 8$)
Demographic and clinical						
Age (years)	64	60	66	67	56	66.2 (12.5)
Sex	F	M	F	F	F	6 F/2 M
Education	16	12	13	16	14	18.2 (2.2)*
Handedness	R	R	L	R	R	6 R/2 L
Years from first symptom	8	7	7	6	3	NA
General cognitive status						
MMSE (30)	22	17	26	29	27	29.6 (0.7)*
CDR total	1	1	0.5	0.5	1	0.0 (0.0)*
Language						
Phonemic fluency	4	9	8	7	9	15.1 (3.1)*
Semantic fluency	3	7	2	4	11	25.6 (5.5)*
Boston naming test (15)	2	3	2	3	4	15 (NA)*
Speech fluency (WAB, 10)	8	8	10	9	9	10 (NA)
Repetition (WAB, 100)	88	NA	92	86	89	NA
Apraxia of speech rating (7)	0	3	0	0	0	0
Dysarthria rating (7)	0	3	0	0	0	0
Word recognition (WAB, 60)	51	51	56	58	57	NA
Peabody picture vocabulary test (16)	2	3	5	6	11	15.7 (0.7)
Sequential commands (WAB, 80)	76	NA	76	72	80	NA
Syntactic comprehension (CYCLE, 55)	53	42	54	52	43	NA
Pyramids and palm trees—Pictures (52)	32	41	34	45	46	NA
Reading						
PALPA Regular words (30)	24	28	20	29	30	NA
PALPA Exception words (30)	13	22	17	23	23	NA
PALPA Pseudowords (24)	37	50	37	52	53	NA
Visuospatial function						
Modified Rey–Osterrieth copy (17)	17	12	15	14	16	15.6 (0.9)
VOSP	10	NA	9	10	10	9.1 (1.3)
Visual memory						
Modified Rey–Osterrieth delay (17)	0	1	11	10	13	12.6 (3.2)*
Verbal memory						
CVLT-MS Trials 1–4	7	4	16	14	20	30.0 (5.9)*
CVLT-MS 30 s free recall	0	0	1	0	4	8.2 (1.3)*
CVLT-MS 10 min free recall	0	1	0	0	4	7.6 (2.6)*
Executive						
Digit span backwards	6	3	4	5	4	4.7 (0.7)
Modified trails lines per minute	11	23	24	49	42	40.0 (15.2)
Calculation	5	4	5	5	4	4.7 (0.5)

Controls' scores are listed as means with SDs in parentheses. Asterisks indicate significantly different values from controls ($P < 0.05$).
F = female; M = male; R = right; L = left; CDR = Clinical Dementia Rating; WAB = Western Aphasia Battery; CYCLE = Curtiss-Yamada Comprehensive Language Examination; PALPA = psycholinguistic assessment of language processing in aphasia; VOSP = Visual Object and Space Perception Battery; CVLT-MS = California Verbal Learning Test-Mental Status.

interest (ROIs) were defined manually on the axial, coronal or sagittal FA images of each subject, and were used as targeting regions for tracking. These ROIs were defined around areas of white matter that are known *a priori* to include the course of each tract (i.e. regions that a tract has to cross to reach its cortical termination). Hence, the use of these white matter regions as targets for tracking allows delineation of all fibres of a single tract without constraining its cortical projections, which may vary from subject to subject, especially when applied to a pathological brain. A one-ROI approach was used to defined the genu and splenium of the corpus callosum (i.e. all fibres passing through the ROI are considered as belonging to a single tract). Since the other tracts share their target regions with one or more tracts, a two-ROI approach was used where a second ROI was defined, such that it contains the desired fasciculus but does not contain any fibres of the undesired fasciculi that passed through the first ROI (Catani and Thiebaut de Schotten, 2008). In detail, the ROIs for the selected tracts were defined as follows:

(i) *Inferior longitudinal fasciculus*. The first ROI was drawn on axial FA slices around the white matter of the ATL. The second ROI was defined on axial FA slices around the occipital white matter lying posterior to the splenium of the corpus callosum. In order to include the entire occipital lobe, coronal and sagittal FA maps were used as reference to identify the parieto-occipital sulcus.

(ii) *Arcuate fasciculus and fronto-parietal superior longitudinal fasciculus.*. A single ROI was drawn on a coronal slice of the colour-coded map to define all of the fibres oriented in an anterior-posterior direction (green on the colour maps), running lateral to the corona radiata and medial to the cortex. Because all the SLF bundles pass through this bottleneck, it is an ideal region to define the main body of the tract (Catani *et al*., 2002; Makris *et al*., 2005; Catani and Thiebaut de Schotten, 2008; Glasser and Rilling, 2008). All the tracts that did not reach the frontal lobe were removed since they represent erroneous tracts or real tracts not meeting our interest in frontally-connected pathways. Then, second ROIs including temporal and parietal regions were selected to perform a detailed dissection of the SLF in its two major segments: the arcuate fasciculus connecting frontal to temporal regions, and the fronto-parietal SLF joining frontal and inferior parietal regions. Temporal ROIs were defined on sagittal FA slices around the entire descending portion of the SLF, corresponding approximately to the posterior third of the superior temporal gyrus, bordered caudally and dorsally by the angular and supramarginal gyri, respectively. We defined the rostral border of the temporal ROIs as the position of the Heschl's gyrus. Parietal ROIs were drawn on axial FA slices around the white matter of the inferior parietal lobe. Sagittal FA maps were used as reference to identify the post-central sulcus (anterior boundary), the intraparietal sulcus (rostral boundary), the parieto-occipital sulcus (dorsal boundary) and the lateral sulcus (lateral boundary).

(iii) *Uncinate fasciculus*. The first ROI was defined as for the ILF. The second ROI was drawn around the white matter of the anterior floor of the external/extreme capsule.

(iv) *Genu and splenium of the corpus callosum.*. Two single horseshoe-shaped ROIs were defined around the genu and the splenium of the corpus callosum.

Anatomical verification of ROIs and tracts

Anatomical verification on structural images allows more accurate anatomical localization of ROIs and tracts than what is possible in the native diffusion space (Basser *et al*., 2000). Extracerebral tissue was removed from the T_1-weighted and the minimally diffusion weighted echo-planar ('$b=0$ volume') images using the brain extraction tool of FSL software (http://www.fmrib.ox.ac.uk/fsl) (Smith, 2002). Then, using FSL, T_1-weighted images were registered linearly to the T_2-weighted volume in the same plane as the DTI data. The registered T_1-weighted images were then registered to the subject's FA space by means of linear and non-linear transformations between the in-plane T_2-weighted (non-echo-planar image)) and $b=0$ DT MRI images. On the resulting T_1-weighted images, the anatomical localization of each subject's ROIs was verified. ROIs that were found to extend outside the expected anatomical structures were edited and re-tracked. Finally, all tracts were reconstructed in 3D using the in-house fibre tracking visualization software (Berman *et al*., 2005), overlaid on the transformed anatomic MRI data sets, and visually checked for consistency with known anatomy.

Defining tract localization

To identify between group differences in tract localization, single subject's tracts were warped into standard Montreal Neurological Institute (MNI) space using FSL, as follows: (i) single subject's T_1-weighted images were linearly and non-linearly normalized to the MNI standard space; (ii) this transformation matrix was applied to single subject's FA maps, previously moved into the T_1 space by inverting and concatenating the linear transformation matrices calculated above and applying nonlinear transformations obtained from warping the echo-planar images to the non-echo-planar image T_2-weighted volumes; (iii) using transformation matrices obtained from these two steps, the binary masks of each subject's tracts were normalized into the standard space. Normalized tract masks were finally superimposed on each other to produce group probabilistic maps.

Deriving tracts-specific DTI metrics

The atrophic changes seen in the grey matter and white matter of patients can cause partial volume effects and, as a consequence, increase the probability of false positive findings. Using the statistical parametric mapping (SPM) 5 software package (Welcome Department of Imaging Neuroscience, London; http://www.fil.ion.ucl.ac.uk/spm) running under Matlab 7.0.1 (Math-Works, Natick, MA, USA), subject's T_1-weighted images were segmented in grey matter, white matter and cerebrospinal fluid (CSF). White matter masks were then thresholded to a value >0.75. Applying the transformation matrices calculated in the previous steps for T_1-weighted images, thresholded white matter masks were normalized to single subject's FA space and then superimposed onto DTI-derived metrics maps. Finally, tract masks were applied to the resulting white matter maps and the tracts' average MD, FA, $\lambda_{//}$ and $\lambda_{\perp}$ were measured. To visually explore the topographical distribution of microstructural damage in each pathway, white matter tracts were also rendered as maps of MD values in all patients and one representative control (Fig. 5). In these maps, MD values are represented in a red-to-white colour scale where lower values are dark red and higher values are yellow to white (Fig. 5).

Statistical analysis

We used linear mixed-effect model analysis (McCulloch *et al*., 2008) to compare simultaneous DTI-derived metrics (MD, FA, $\lambda_{//}$ and $\lambda_{\perp}$) between semantic dementia patients and controls for each tract. We fit separate models for each DTI variable. Specifically, these models contained predictors for Group, Tract and the Tract $\times$ Group interaction, as well as age as an additional covariate. The models also contained random intercepts to accommodate the correlation between the responses at multiple tracts within the same subject. The coefficients of Group and the Tract $\times$ Group interaction measure the tract-specific group differences for each DTI variable. Testing that these coefficients are all zero provides an overall, multivariate test of the hypothesis that the group-specific means of a given variable are the same for each of the four tracts studied. We conducted these multivariate tests using the Wald approach. Then, we assessed tract-specific differences in each DTI variable using a Fisher's Least Significant Difference approach (Miller, 1981). We first carried out the overall, multivariate test described earlier. If we rejected this multivariate hypothesis at $\alpha=0.05$, then we conducted tract-specific tests, each at $\alpha=0.05$, and constructed 95% confidence intervals for tract-specific differences in group means. If we did not reject the multivariate hypothesis at $\alpha=0.05$, then we did not proceed to the second stage. We fit all the linear mixed-effects models and carried out all hypothesis tests using routines in Stata (Stata Statistical Software: Release 10. College Station, TX: StataCorp LP).

fMRI

Functional imaging data were analysed with SPM5 (Wellcome Department of Imaging Neuroscience, London; http://www.fil.ion.ucl.ac.uk/spm). Briefly, the preprocessing steps were slice timing correction, realignment to correct for within-scan head movement, coregistration of the mean functional image to a T_1 structural image acquired during the pre-existing protocol, nonlinear warping of these coregistered images to the atlas space of the MNI, and smoothing with a Gaussian kernel of 8 mm full width at half maximum. In each of the two runs, subjects were asked to read out loud 10 high-frequency regular words, 10 low-frequency regular words, 10 high-frequency exception words, 10 low-frequency exception words, 10 pseudowords and 10 false font strings as reported by Wilson *et al*. (2009). For this study, we performed two new analyses to identify: (i) brain regions involved in reading words that stress the whole-word reading process in the control group and semantic dementia patients, considering high-frequency regular words, high-frequency exception words, low-frequency exception words versus rest; and (ii) brain regions involved in sublexical reading processes in the control group and semantic dementia patients, considering low-frequency regular words, and pseudowords versus rest. Random effects *t*-statistics were thresholded at $t > 2.5$ to enable visualization of frontal and parietal activated regions. More details on the design and analysis of the fMRI experiment, including determination of statistical significance for particular clusters, have been previously reported (Wilson *et al*., 2009).

Voxel-based morphometry

Voxel-based morphometry analysis included two steps: spatial preprocessing (normalization, segmentation, Jacobian modulation and smoothing) and statistical analysis (Ashburner and Friston, 2000; Good *et al*., 2002). Both stages were performed using SPM5. T_1-weighted images were segmented, normalized into the MNI space, and modulated using the unified segmentation model (Ashburner and Friston, 2005). The final voxel resolution after normalization was $2.0 \times 2.0 \times 2.0\,mm^3$. Spatially normalized, modulated grey matter and white matter images were then smoothed with a 12-mm full width at half maximum isotropic Gaussian kernel. A general linear model was then fit at each voxel to compare grey matter and white matter between patients with controls. Age, gender and total intracranial volume were confounding variables. The resulting statistical parametric maps were thresholded voxelwise at $P < 0.001$, and then only clusters significant at $P < 0.05$ (corrected based on Gaussian Random Field theory) were retained. Correction for non-stationary smoothness was applied (Hayasaka *et al*., 2004), using the implementation of this method in the voxel-based morphometry-5 toolbox (http://dbm.neuro.uni-jena.de/vbm), as is necessary to avoid false positives with voxel-based morphometry. Results are presented only for the white matter analysis since the grey matter results have been reported elsewhere (Wilson *et al*., 2009).

Results

Demographic, clinical and cognitive data

There were no significant differences between groups in age, sex and handedness. Semantic dementia patients had lower education, MMSE and Clinical Dementia Rating Scale scores compared with controls. On the general neuropsychological screening, patients were impaired on verbal and nonverbal episodic memory, while they did not differ significantly from controls on visuospatial, executive and calculation tasks performance. On language testing, semantic dementia patients showed the typical pattern of impairment, with severe difficulty in single word comprehension, naming, semantic association and irregular word reading tasks with relative sparing in fluency, grammar and phonological tasks. The neuropsychological profile of these patients is shown in Table 1 for completeness.

Voxel-based morphometry

In semantic dementia patients, white matter volumes were significantly different from controls in the left ATL including the more medial portion ($P < 0.05$, corrected at the cluster level) (Fig. 1). white matter atrophy was thus located underneath the left

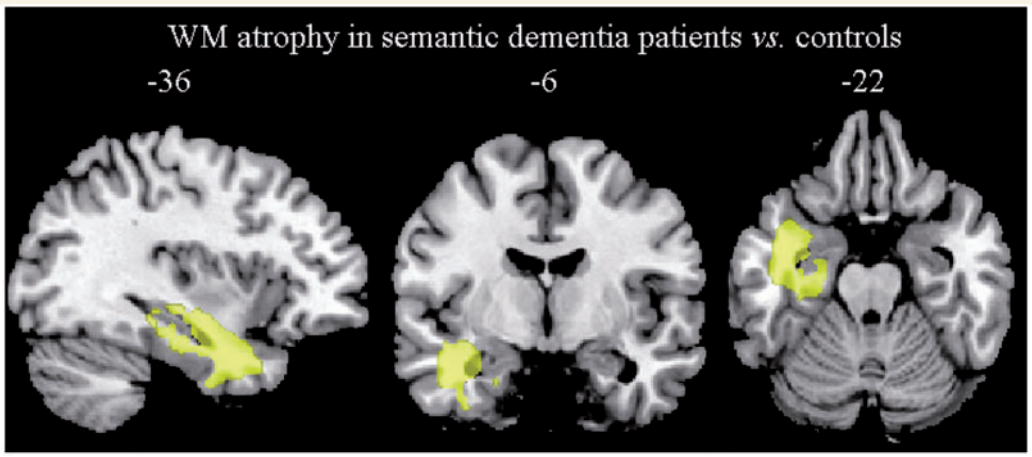

Figure 1 The pattern of white matter atrophy in patients with semantic dementia compared with 48 age-matched healthy controls ($P < 0.05$, corrected at the cluster level). Regions are superimposed on the MNI standard brain in neurological convention (right is right) WM = white matter.

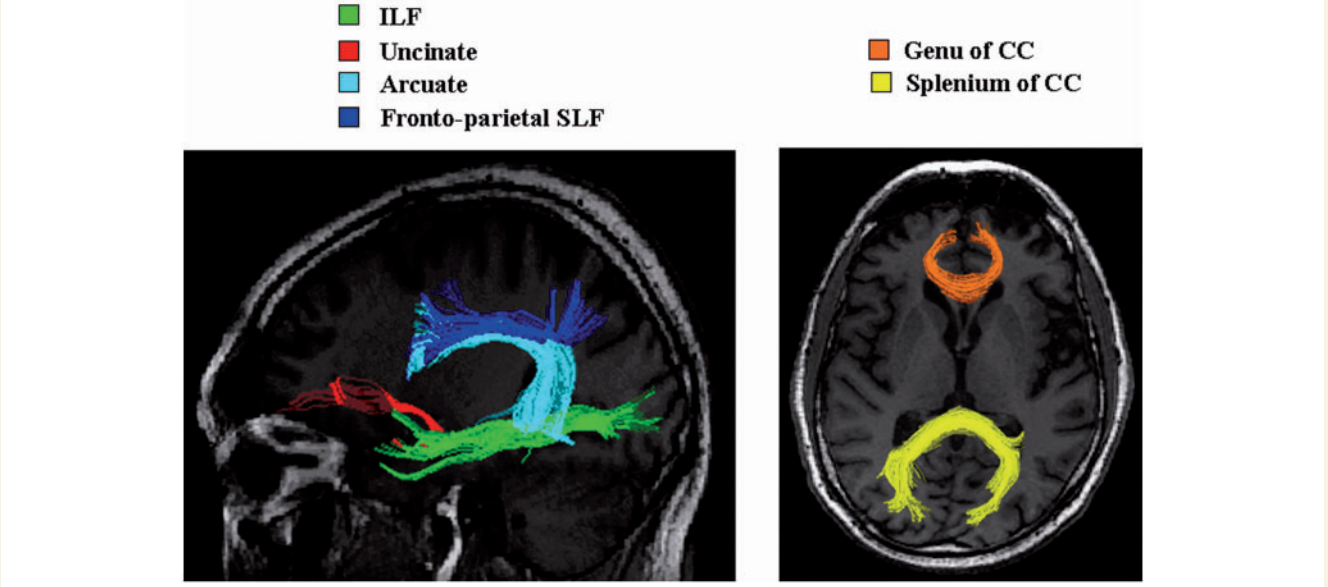

Figure 2 Reconstructions of white matter tracts in a single healthy control: the left ILF in green, the left uncinate fasciculus in red, the left arcuate fasciculus in cyan, the left fronto-parietal SLF in blue, the genu of the corpus callosum in orange and the splenium of the corpus callosum in yellow. Tracts are superimposed onto the subject's T_1-weighted image normalized into the FA space. CC = corpus callosum

temporal cortical regions that are most often involved in semantic dementia in general and in this group in particular (Wilson *et al*., 2009).

DTI data

Anatomical localization of white matter tracts

Figure 2 shows an example of the reconstructed trajectories of the white matter tracts of a single healthy control. Probabilistic maps of these tracts were created to investigate the consistency of distribution of the identified pathways in the two groups (Figs 3 and 4). Visual assessment of these maps showed a consistent and similar pattern of connections in the two groups.

The left ILF was successfully identified in all subjects. Within the larger ROIs used to detect the tract, the left ILF pathway consistently linked the entire temporal pole [Brodmann areas (BAs) 20, 21, 38] to the regions underlying the associative occipital cortices (BA 18 and 19) (Fig. 3).

The left arcuate was found in all subjects and consistently connected the posterior part of the STG (BA 22) and the middle temporal gyrus (BA 21 and 37) to the posterior, opercular portion of the inferior frontal gyrus (BA 44) and the precentral (BA 6) region in the frontal lobe (Fig. 3). In one control and one patient (Case 3), the frontal projection of the left arcuate also terminated in the more anterior portion close to the inferior frontal gyrus (BA 45).

As described earlier (Catani *et al*., 2007), the left fronto-parietal SLF was less consistently found than other tracks and was present in six of eight controls and all patients. This pathway consistently connected the supramarginal (BA 40) and the angular (BA 39) area to the inferior frontal (BA 44) and the precentral (BA 6) gyri (Fig. 3). In one patient (Case 3), its frontal projection also terminated in the more anterior inferior frontal region (BA 45).

The left uncinate fasciculus was successfully reconstructed in all controls and four of five semantic dementia patients. Fibre tracking failed in Case 1 because of severe atrophy and distortion in the medial ATL that precluded the reconstruction of the temporal component of the tract. In all other subjects, the identified uncinate fasciculus consistently connected the anterior, medial temporal lobe (BA 20 and 38) to the white matter surrounding the orbital frontal cortex (BAs 11 and 47) (Fig. 3).

The genu and splenium of the corpus callosum were successfully reconstructed in all subjects. The anterior portion (genu) consistently connected the prefrontal and orbitofrontal regions (BAs 10 and 11), while the posterior portion (splenium) consistently connected the occipital and parietal lobes (BAs 7 and 18) (Fig. 4).

Tract-specific DTI-derived metrics

Table 2 shows the DTI-derived metrics of each tract from each semantic dementia patient as well as the mean values from patient and control groups. The multivariate tests simultaneously comparing the four tract-specific means of all the DTI-derived metrics found that MD ($\chi^2 = 44.05$, $P < 0.001$), FA ($\chi^2 = 33.02$, $P < 0.001$), $\lambda_{//}$ ($\chi^2 = 32.28$, $P < 0.001$), and $\lambda_{\perp}$ ($\chi^2 = 33.88$, $P < 0.001$) were significantly different between patients and controls. The Fisher Least Significant Difference test showed that semantic dementia patients had significantly higher MD, $\lambda_{//}$ and $\lambda_{\perp}$ in the left ILF compared with controls (Table 2). Relative to controls, the left uncinate and arcuate fasciculi demonstrated significantly higher MD, $\lambda_{//}$ and $\lambda_{\perp}$, and significantly lower FA, while the left fronto-parietal SLF had significantly higher $\lambda_{\perp}$ and significantly lower FA, only (Table 2). In the corpus callosum, the genu

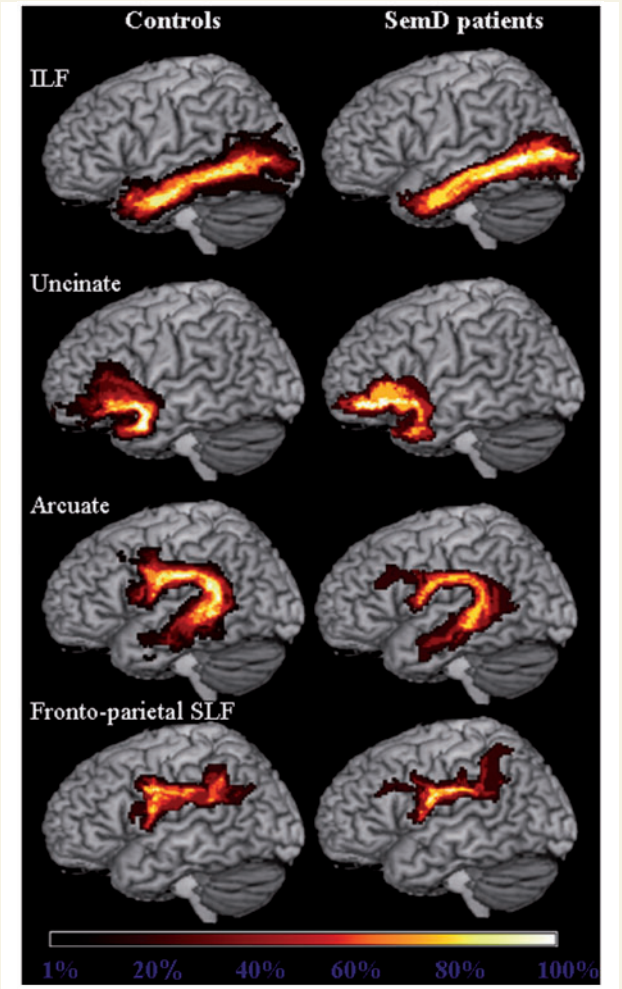

Figure 3 Group probabilistic maps of the language-related white matter tracts from healthy controls and semantic dementia (SemD) patients. Left ILF, uncinate fasciculus, arcuate fasciculus and fronto-parietal SLF are superimposed on the three-dimensional rendering of the MNI standard brain. The colour scale indicates the degree of overlap among subjects.

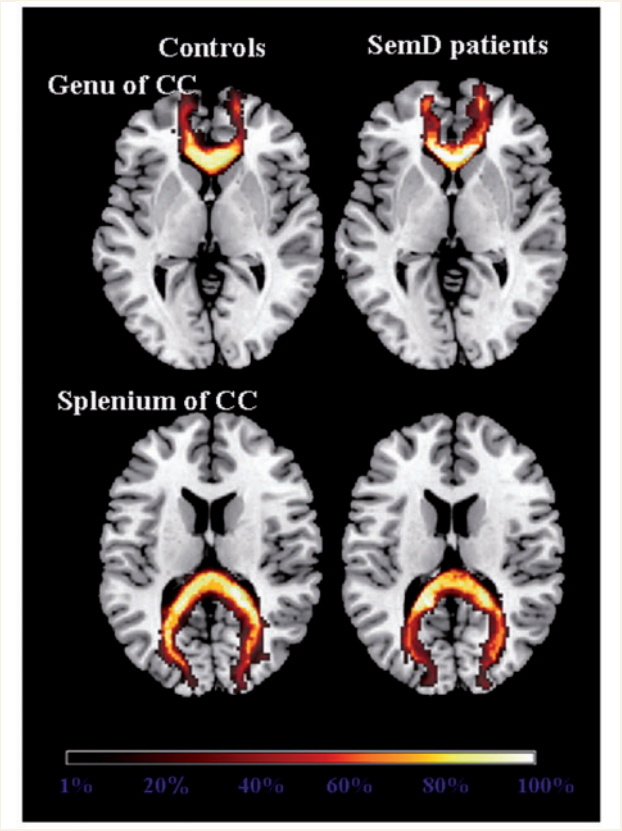

Figure 4 Group probabilistic maps of the genu and splenium of the corpus callosum from healthy controls and semantic dementia (SemD) patients are shown on the axial sections of the MNI standard brain. The colour scale indicates the degree of overlap among subjects.

showed significantly lower FA compared with controls, while no between-group difference was found in the splenium (Table 2). As shown in Fig. 5, more severe damage (i.e. higher MD values) was present in the anterior portion of the ILF and the portion of the arcuate and uncinate fasciculi located in the temporal pole.

fMRI data

The first fMRI analysis showed that semantic dementia patients had reduced activation in the mid-fusiform gyrus or the superior temporal gyrus for words versus rest when compared to controls. These regions overlapped areas of grey matter atrophy in the patient group (Wilson *et al.*, 2009) and correspond to regions linked through the ILF and the arcuate fasciculus. Sublexical reading fMRI analysis demonstrated that reading areas in left intraparietal sulcus and posterior inferior frontal gyrus were either normally activated in semantic dementia patients, or hyperactivated in some cases compared to controls (i.e. reading of low-frequency exception words). These regions corresponded to the grey matter areas that are connected by the fronto-parietal SLF that also was relatively spared in our DTI study. Figure 6 highlights this anatomical correspondence by showing the fronto-parietal SLF probability map and activation maps obtained in control subjects and semantic dementia patients for a contrast which highlights sublexical processing: low frequency regular words and pseudowords versus rest. The regions at either end of the fronto-parietal SLF were activated in semantic dementia patients to the same extent as in control subjects, consistent with the functional integrity of the tract and the grey matter areas it connects.

Post hoc correlation analyses between white matter tracts damage and cognitive variables

Post hoc exploratory analyses were performed to investigate the relationship between damage to language-related white matter tracts and the semantic and sublexical, phonological components of the cognitive deficits in semantic dementia patients. Univariate

Table 2 DTI-derived metrics for white matter tracts for each semantic dementia patient with means for the two study groups

		Case 1	Case 2	Case 3	Case 4	Case 5	Patients, mean (SD)	Controls, mean (SD)	*P*-values
ILF	MD	0.77	0.76	0.72	0.73	0.66	0.73 (0.05)	0.67 (0.01)	<0.001
	FA	0.29	0.32	0.32	0.31	0.33	0.31 (0.01)	0.32 (0.01)	0.20
	$\lambda_{//}$	1.04	1.04	0.98	1.00	0.91	0.99 (0.06)	0.92 (0.02)	<0.001
	$\lambda_{\perp}$	0.64	0.63	0.59	0.60	0.53	0.60 (0.04)	0.55 (0.01)	<0.001
Arcuate	MD	0.68	0.71	0.66	0.62	0.59	0.65 (0.05)	0.60 (0.01)	0.002
	FA	0.30	0.32	0.32	0.33	0.34	0.32 (0.02)	0.34 (0.02)	0.001
	$\lambda_{//}$	0.91	0.97	0.89	0.84	0.82	0.89 (0.06)	0.84 (0.02)	0.01
	$\lambda_{\perp}$	0.57	0.58	0.62	0.50	0.48	0.53 (0.04)	0.49 (0.01)	<0.001
Fronto- parietal SLF	MD	0.64	0.65	0.66	0.61	0.60	0.63 (0.03)	0.61 (0.01)	0.09
	FA	0.28	0.31	0.30	0.28	0.32	0.30 (0.02)	0.32 (0.02)	0.001
	$\lambda_{//}$	0.83	0.88	0.87	0.80	0.81	0.84 (0.04)	0.82 (0.02)	0.45
	$\lambda_{\perp}$	0.47	0.54	0.55	0.52	0.49	0.53 (0.02)	0.50 (0.01)	0.02
Uncinate	MD	NA	0.87	0.75	0.73	0.71	0.77 (0.07)	0.67 (0.02)	<0.001
	FA	NA	0.26	0.28	0.27	0.27	0.27 (0.01)	0.31 (0.01)	<0.001
	$\lambda_{//}$	NA	1.11	0.98	0.96	0.93	1.00 (0.08)	0.91 (0.02)	<0.001
	$\lambda_{\perp}$	NA	0.66	0.64	0.62	0.60	0.65 (0.07)	0.56 (0.02)	<0.001
Genu of the corpus callosum	MD	0.73	0.80	0.80	0.74	0.72	0.76 (0.04)	0.73 (0.02)	0.85
	FA	0.34	0.32	0.37	0.33	0.33	0.34 (0.02)	0.35 (0.01)	0.02
	$\lambda_{//}$	1.03	1.10	1.16	1.03	1.00	1.06 (0.06)	1.04 (0.03)	0.08
	$\lambda_{\perp}$	0.58	0.64	0.62	0.59	0.58	0.60 (0.03)	0.58 (0.02)	0.77
Splenium of the corpus callosum	MD	0.77	0.67	0.71	0.68	0.66	0.70 (0.04)	0.71 (0.03)	0.51
	FA	0.38	0.38	0.39	0.37	0.37	0.38 (0.01)	0.38 (0.01)	0.17
	$\lambda_{//}$	1.12	0.98	1.05	0.98	0.94	1.01 (0.07)	1.04 (0.05)	0.15
	$\lambda_{\perp}$	0.59	0.52	0.54	0.53	0.51	0.54 (0.03)	0.55 (0.02)	0.32

MD, $\lambda_{//}$ and $\lambda_{\perp}$ values are $\times 10^{-3}\,mm^2\,s^{-1}$.
NA = not applicable.
P-values refer to Fischer Least Significant Difference Test.

correlations were assessed between tracts MD values and the correspondent cognitive scores using the Spearman rank correlation coefficient. Correlation analyses were performed with Statistical Package for the Social Sciences (SPSS) (version 16.0 for Windows; SPSS Inc., Chicago, IL). The left ILF and arcuate MD values significantly correlated with Peabody Picture Vocabulary test total score (Spearman's $\rho = -0.90$, $P = 0.04$). The Spearman's ρ for the correlation between left ILF and arcuate MD and semantic fluency score, Boston naming test (BNT) score, word recognition (Western Aphasia Battery—WAB) score and Pyramids and palm trees-Pictures score ranged from −0.30 to −0.87; however they were not statistically significant. The left fronto-parietal SLF MD was significantly correlated with the PALPA (Psycholinguistic Assessments of Language Processing in Aphasia) regular words score (Spearman's $\rho = -0.90$, $P = 0.04$).

Discussion

In this study, we used a multimodal imaging approach to investigate the integrity of language networks in semantic dementia. We found that semantic dementia was associated with greater damage of the connections that pass through the temporal lobe (i.e. the ILF, the uncinate fasciculus and the arcuate fasciculus), while the fronto-parietal connection (i.e. the fronto-parietal SLF) and the corpus callosum were less involved. The DTI results were consistent with volumetric and functional sparing of the same networks as measured by voxel-based morphometry and fMRI. We discuss these findings in relation to previous literature and current models of language processing.

It is common knowledge that semantic dementia is associated with ATL and ventromedial frontal grey matter atrophy (Mummery *et al*., 2000; Galton *et al*., 2001; Rosen *et al*., 2002; Gorno-Tempini *et al*., 2004) but limited evidence is available regarding microstructural white matter damage. Only a few DTI-based studies are published in primary progressive aphasia and related disorders (Larsson *et al*., 2004; Borroni *et al*., 2007; Matsuo *et al*., 2008), and even fewer using the most recent tractography analysis methods (Matsuo *et al*., 2008). In a single, pathology-proven, frontotemporal dementia case, ROI-based DTI showed decreased FA in frontal regions, where histopathology revealed typical frontal lobe degeneration of non-Alzheimer's disease type (Larsson *et al*., 2004). To our knowledge, the only published whole-brain, voxel-based DTI study in patients with semantic dementia showed an FA decrease in several temporal and frontal regions (Borroni *et al*., 2007), but because of the nature of the voxel-based analysis method, the study could only infer which specific tracts were involved. DTI-based tractography is instead needed for the direct localization and the quantitative assessment of DTI metrics within specific neuronal pathways (Conturo *et al*., 1999; Basser *et al*., 2000; Wakana *et al*., 2004; Catani and Thiebaut de Schotten, 2008). Quantitative

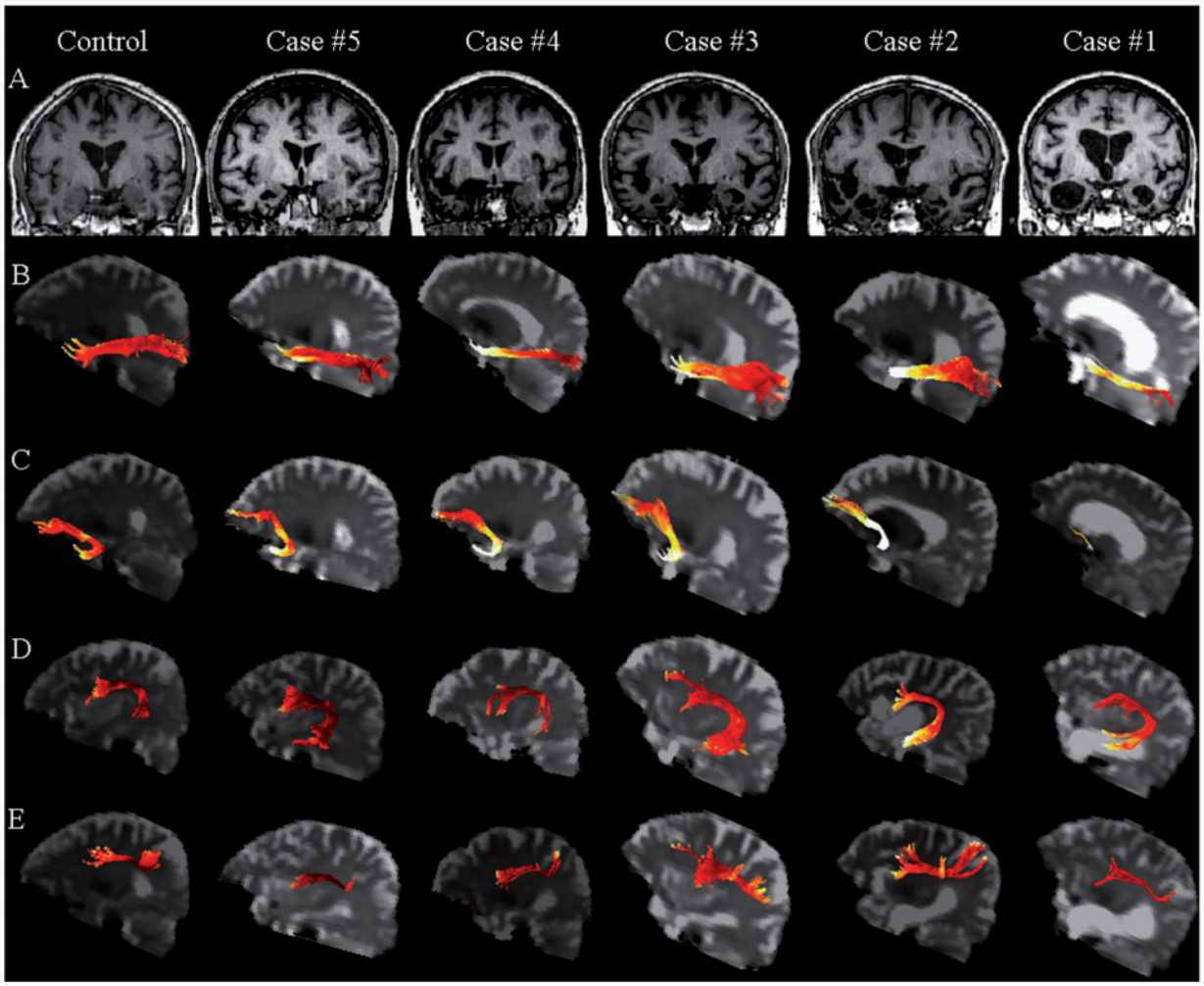

Figure 5 (**A**) Structural MRI of one representative control and each semantic dementia patient (coronal view). (**B**–**D**) Left language-related white matter tracts are rendered as maps of MD in one representative control and all patients (**B**: ILF; **C**: uncinate fasciculus; **D**: arcuate fasciculus; **E**: fronto-parietal SLF). The colour scale represents the MD values going from lower (dark red) to higher values (yellow to white). Maximum damage is present in the anterior portion of the ILF and uncinate fasciculus underlying the temporal pole.

tractography studies successfully examined the microstructure of white matter in neurodegenerative diseases (Xie *et al*., 2005; Taoka *et al*., 2006; Ciccarelli *et al*., 2008; Damoiseaux *et al*., 2008), and more recently in frontotemporal dementia (Matsuo *et al*., 2008; Zhang *et al*., 2009). The study of Matsuo *et al*. (2008) included semantic dementia patients within a larger clinical behavioural frontotemporal dementia group, and showed a significant FA decrease in all major association fibres (ILF, uncinate and arcuate) and in the genu of the corpus callosum, with sparing of the pyramidal tracts and splenium of the corpus callosum. The authors did not investigate group differences between clinical variants (Matsuo *et al*., 2008) and it was therefore not clear which tracts were related to semantic dementia. Our findings are consistent with these previous studies and add new insight into the localization and relative severity of white matter tract involvement. As in frontotemporal dementia,, the uncinate fasciculus (Matsuo *et al*., 2008; Zhang *et al*., 2009), the arcuate fasciculus and the ILF (Matsuo *et al*., 2008) were affected in semantic dementia. Interestingly, all the white matter tracts that run to the temporal lobe demonstrated increases in MD, $\lambda_{//}$ and $\lambda_{\perp}$. This pattern of DTI changes has been previously reported with ageing (Sullivan *et al*., 2008; Vernooij *et al*., 2008) and is thought to reflect a combination of decreased axonal packing in white matter structures and demyelination, allowing for increased diffusivity in all orientations within a voxel. The lack of FA changes in ILF could appear unexpected, however, if changes along the direction of the major axis of the diffusion ellipsoid ($\lambda_{//}$) were proportional to those of the minor axes ($\lambda_{\perp}$), then FA, which is a function of the ratio between parallel to transverse diffusivities, can remain relatively unchanged (Basser *et al*., 1994). This is likely to be the case in the ILF. Within all temporal tracts, MD values were most abnormal in the ATL (Fig. 5). In contrast to the severe involvement of temporal tracts, the left fronto-parietal SLF was the least affected in semantic dementia, as indicated by the modest

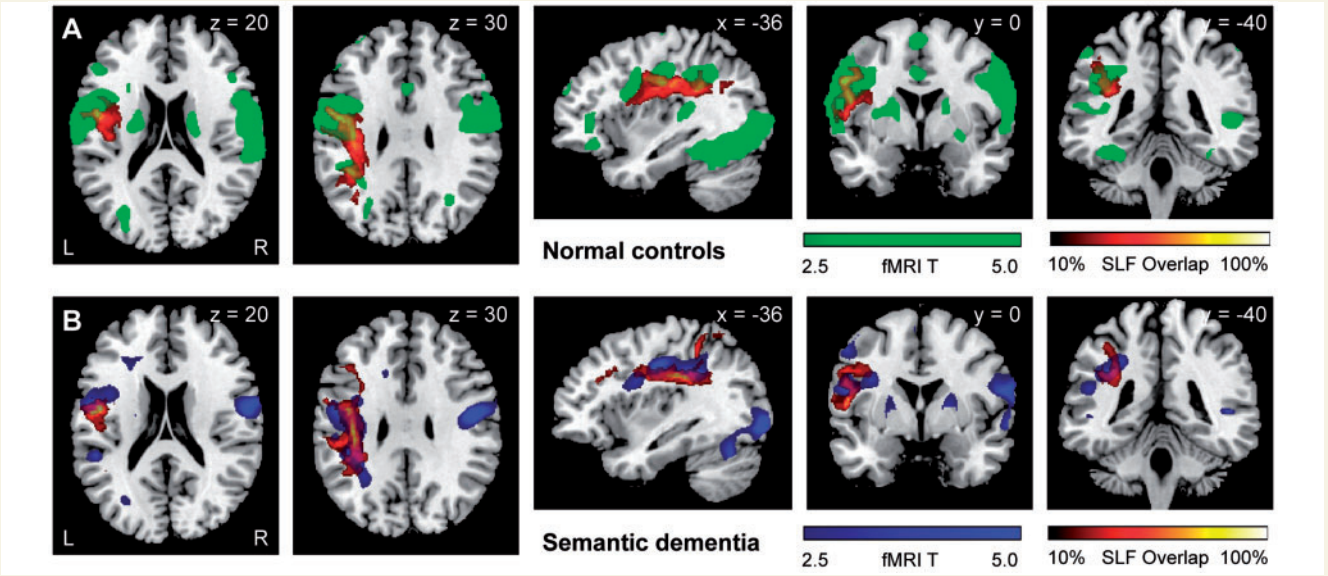

Figure 6 Anatomical correspondence between fronto-parietal SLF and activation for a contrast which highlights sublexical processing in control subjects (**A**) and semantic dementia patients (**B**). fMRI activations for the contrast of low-frequency regular words and pseudowords versus rest are shown in green (**A**) for healthy controls and in blue (**B**) for semantic dementia patients. The healthy control group and the semantic dementia patients both showed activation of posterior inferior frontal gyrus and inferior parietal cortex. Probabilistic maps of the left fronto-parietal SLF obtained in healthy controls (**A**) and semantic dementia patients (**B**) are shown in a colour scale which indicates the degree of overlap among subjects. Results are superimposed on the MNI standard brain in neurological convention (right is right).

decrease in FA in the context of normal MD values (due to the increase in $\lambda_{\perp}$, only). This is consistent with the semantic dementia clinical picture (see below) and with previous anatomical evidence that inferior parietal grey matter and white matter regions are more affected in Alzheimer's disease than in frontotemporal dementia-related disorders (Chao *et al*., 2007; Rabinovici *et al*., 2007). The pattern of DTI changes in the corpus callosum is consistent with previous structural MRI (Yamauchi *et al*., 2000) and DTI tractography (Matsuo *et al*., 2008; Zhang *et al*., 2009) studies in frontotemporal dementia.

The functional anatomy of language-related white matter tracts is currently a matter of active research and the relative roles of grey matter and white matter are still debated (for review see Catani and Mesulam, 2008; Duffau, 2008). Our results, taken together with previous data (Mummery *et al*., 1999; Sonty *et al*., 2007; Wilson *et al*., 2009), suggest that a grey matter and white matter dysfunction in the ventral semantic pathway, combined with a relative sparing of a more dorsal fronto-parietal sublexical, phonological pathway, are responsible for the unique combination of impaired and spared language domains that is typical of semantic dementia and never observed in stroke-induced aphasia. The combination of cortical ATL and ILF damage, with sparing of posterior visual cortex, are likely to be responsible for the 'disconnection' between degraded multimodal semantic representations (in ATL) and normal visual perceptual functions (in associative visual cortex) that is typical of semantic dementia. For instance, semantic dementia patients usually perceive faces normally, but have severe person identification deficits when asked to retrieve semantic information from known faces or proper names (Patterson and Hodges, 1992; Hodges and Patterson, 1996; Gorno-Tempini *et al*., 2004). The relative sparing of the fronto-parietal network (inferior parietal cortex and the fronto-parietal SLF) could explain the relative preservation of fluency, grammar and sublexical phonological processes (see, for instance, our Case 3 that showed the severe difficulty in naming with a BNT of 2 in the context of a normal WAB fluency score of 10) (Patterson and Hodges, 1992; Hodges and Patterson, 1996; Gorno-Tempini *et al*., 2004). This hypothesis is supported by the fMRI reading findings. The left mid-fusiform gyrus and superior temporal regions were less activated in patients with semantic dementia, showed significant grey matter atrophy and were connected by damaged white matter tracts (i.e. ILF and arcuate). On the other hand, semantic dementia patients showed a normal activation of the posterior inferior frontal gyrus and inferior parietal cortices when reading words that stress sublexical processes (Fig. 6). Furthermore, these areas were not significantly atrophied and were connected by the spared fronto-parietal SLF. In relation to reading, our results are consistent with previous findings (Perani *et al*., 1999; Silani *et al*., 2005) in suggesting that the structural and functional impairment of the temporal grey matter regions, together with the damage to the ILF and arcuate fasciculus, cause deficits in retrieval of exceptional, item-specific word forms, while the functional and structural sparing of the inferior parietal and fronto-parietal SLF pathway subserve spared sublexical, phonological processes. This unique dissociation between the temporal and fronto-parietal language networks does not usually occur in stroke and could thus be responsible for the unusual combination of spared and impaired functions in semantic dementia

The clinical correlate of the damaged arcuate fasciculus needs further investigation. Classically, injury to the arcuate is considered to be the anatomical basis for repetition deficits in vascular conduction aphasia (Goodglass *et al*., 1964). Yet, despite damage to the arcuate, repetition is typically spared in our group and in semantic dementia in general (Patterson and Hodges, 1992; Hodges and Patterson, 1996; Gorno-Tempini *et al*., 2004) making this hypothesis less probable. Recent studies indeed highlight the role of cortical inferior parietal and posterior temporal structures in repetition (Selnes *et al*., 1985; Baldo and Dronkers, 2006; Gorno-Tempini *et al*., 2008). Future studies, combining a DTI voxel-based approach within the arcuate fasciculus and grey matter analysis, will further clarify the anatomic substrate of repetition deficits and the specific functions of the arcuate fasciculus.

The functional role of the uncinate fasciculus in language processing is still debated. It has been suggested that it may be associated with lexical retrieval, semantic association and aspects of naming that require connections from temporal to frontal components of the language network (Lu *et al*., 2002; Grossman *et al*., 2004; Catani and Mesulam, 2008), even though its termination within the frontal lobe seems to be centred in the ventral and orbital regions (Catani *et al*., 2002; Catani and Thiebaut de Schotten, 2008). This anatomical distribution suggests that injury to the uncinate is likely to be responsible for the behavioural, more than linguistic, symptoms of the semantic dementia, such as loss of empathy, disinhibition and change in personality and compulsive behaviours (Rosen *et al*., 2006). This hypothesis is supported by recent findings of a damaged uncinate in frontotemporal dementia (Matsuo *et al*., 2008; Zhang *et al*., 2009) and by a previous voxel-based DTI study showing the association between medial and ventral frontal white matter damage and behavioural symptoms in these patients (Borroni *et al*., 2007). It is also worth noting that the involvement of the uncinate fasciculus is a well-known feature in Alzheimer's disease (Taoka *et al*., 2006; Yasmin *et al*., 2008; Zhang *et al*., 2009). In the ATL, the uncinate contains cholinergic fibres from the basal nucleus of Meynert. Furthermore, the disruption in connectivity between the temporal and frontal lobes via the uncinate fasciculus has been postulated as a possible cause of posttraumatic retrograde amnesia (Levine *et al*., 1998).

Taken together, DTI, voxel-based morphometry and fMRI findings suggest that a network-level dysfunction in the language system is responsible for the combination of impaired and spared functions typical of the semantic dementia clinical syndrome. This interpretation is congruent with recent cognitive models of language processing and with the vulnerability hypothesis of neurodegenerative diseases (Seeley, 2008). Indeed, recent theoretical models of language functioning propose that different anatomical 'streams' within the ventral and dorsal left hemisphere, are involved in different aspects of language processing (Hickok and Poeppel, 2004, 2007). Our results confirm that semantic dementia is linked to a specific vulnerability of the ventral semantic processing stream of the temporal lobe.

The main limitation of this study is the small patient sample. However, all five patients showed fairly similar results and our sample was adequate to show significant microstructural changes in expected regions within the language network. Furthermore, it must be remembered that semantic dementia is a rare disorder, this multimodal imaging study was characterized by a long MRI acquisition time (which may be challenging in too behaviourally impaired patients), and few previous functional studies on semantic dementia involved small numbers of subjects. A methodological problem relates to the fact that cortical and white matter atrophic changes may cause partial volume effects from the CSF in DT images and consequently increase the probability of false positive findings. In our DTI analysis, precautions were taken to ensure that this may not have influenced the results much and contamination from the CSF was minimized by deriving DTI-based metrics from white matter tracts after CSF masking and white matter thresholding. Furthermore, it has to be considered that partial volume effect should have influenced MD and FA values in concert, which is not the case in the left ILF.

In conclusion, this study shows that the *in vivo* assessment of language-related white matter pathways in patients with semantic dementia using a multi-modal imaging approach combining structural MRI, DTI-based tractography and fMRI is not only feasible but also holds significant promise to gain additional insight into the role of the language network changes in semantic dementia symptoms pathogenesis. Further investigations involving larger groups of subjects, possibly early in the disease course, are now warranted to confirm these findings and to investigate whether the involvement of white matter networks, along with grey matter loss, is related to the different clinical symptoms associated with semantic dementia.

Acknowledgements

The authors thank Victoria Beckman, Lovingly Quitania, Linda Isaac, Jung Jang and Matthew Growdon for administrative support, SungWon Chung and Serena Amici for scientific collaboration and all the patients and healthy volunteers who participated in the study.

Funding

National Institutes of Health (NINDS R01 NS050915, NIA P50 AG03006, NIA P01 AG019724); State of California (DHS 04-35516); Alzheimer's Disease Research Center of California (03-75271 DHS/ADP/ARCC); Larry L. Hillblom Foundation; John Douglas French Alzheimer's Foundation; Koret Family Foundation; McBean Family Foundation.

References

Ashburner J, Friston KJ. Voxel-based morphometry—the methods. NeuroImage 2000; 11: 805–21.

Ashburner J, Friston KJ. Unified segmentation. NeuroImage 2005; 26: 839–51.

Baldo JV, Dronkers NF. The role of inferior parietal and inferior frontal cortex in working memory. Neuropsychology 2006; 20: 529–38.

Basser PJ, Mattiello J, LeBihan D. Estimation of the effective self-diffusion tensor from the NMR spin echo. J Magn Reson B 1994; 103: 247–54.

Basser PJ, Pajevic S, Pierpaoli C, Duda J, Aldroubi A. In vivo fiber tractography using DT-MRI data. Magn Reson Med 2000; 44: 625–32.

Beaulieu C. The basis of anisotropic water diffusion in the nervous system – a technical review. NMR Biomed 2002; 15: 435–55.

Berman JI, Mukherjee P, Partridge SC, Miller SP, Ferriero DM, Barkovich AJ, et al. Quantitative diffusion tensor MRI fiber tractography of sensorimotor white matter development in premature infants. NeuroImage 2005; 27: 862–71.

Borroni B, Brambati SM, Agosti C, Gipponi S, Bellelli G, Gasparotti R, et al. Evidence of white matter changes on diffusion tensor imaging in frontotemporal dementia. Arch Neurol 2007; 64: 246–51.

Catani M, Thiebaut de Schotten M. A diffusion tensor imaging tractography atlas for virtual in vivo dissections. Cortex 2008; 44: 1105–32.

Catani M, Mesulam M. The arcuate fasciculus and the disconnection theme in language and aphasia: history and current state. Cortex 2008; 44: 953–61.

Catani M, Howard RJ, Pajevic S, Jones DK. Virtual in vivo interactive dissection of white matter fasciculi in the human brain. NeuroImage 2002; 17: 77–94.

Catani M, Jones DK, Donato R, Ffytche DH. Occipito-temporal connections in the human brain. Brain 2003; 126: 2093–107.

Catani M, Allin MP, Husain M, Pugliese L, Mesulam MM, Murray RM, et al. Symmetries in human brain language pathways correlate with verbal recall. Proc Natl Acad Sci USA 2007; 104: 17163–8.

Chao LL, Schuff N, Clevenger EM, Mueller SG, Rosen HJ, Gorno-Tempini ML, et al. Patterns of white matter atrophy in frontotemporal lobar degeneration. Arch Neurol 2007; 64: 1619–24.

Ciccarelli O, Catani M, Johansen-Berg H, Clark C, Thompson A. Diffusion-based tractography in neurological disorders: concepts, applications, and future developments. Lancet Neurol 2008; 7: 715–27.

Conturo TE, Lori NF, Cull TS, Akbudak E, Snyder AZ, Shimony JS, et al. Tracking neuronal fiber pathways in the living human brain. Proc Natl Acad Sci U S A 1999; 96: 10422–7.

Damoiseaux JS, Smith SM, Witter MP, Arigita EJ, Barkhof F, Scheltens P, et al. White matter tract integrity in aging and Alzheimer's disease. Hum Brain Mapp 2009; 30: 1051–9.

Davies RR, Hodges JR, Kril JJ, Patterson K, Halliday GM, Xuereb JH. The pathological basis of semantic dementia. Brain 2005; 128: 1984–95.

Dejerine J. Anatomie des centres nerveux. In: Rueff et Cie, editor. Rueff et Cie. Paris; 1895.

Duffau H. The anatomo-functional connectivity of language revisited. New insights provided by electrostimulation and tractography. Neuropsychologia 2008; 46: 927–34.

Galton CJ, Patterson K, Graham K, Lambon-Ralph MA, Williams G, Antoun N, et al. Differing patterns of temporal atrophy in Alzheimer's disease and semantic dementia. Neurology 2001; 57: 216–25.

Glasser MF, Rilling JK. DTI Tractography of the human brain's language pathways. Cereb Cortex 2008; 18: 2471–82.

Good CD, Scahill RI, Fox NC, Ashburner J, Friston KJ, Chan D, et al. Automatic differentiation of anatomical patterns in the human brain: validation with studies of degenerative dementias. NeuroImage 2002; 17: 29–46.

Goodglass H, Quadfasel FA, Timberlake WH. Phrase length and type and severity of aphasia. Cortex 1964; 1: 133–53.

Gorno-Tempini ML, Murray RC, Rankin KP, Weiner MW, Miller BL. Clinical, cognitive and anatomical evolution from nonfluent progressive aphasia to corticobasal syndrome: a case report. Neurocase 2004; 10: 426–36.

Gorno-Tempini ML, Brambati SM, Ginex V, Ogar J, Dronkers NF, Marcone A, et al. The logopenic/phonological variant of primary progressive aphasia. Neurology 2008; 71: 1227–34.

Grossman M, McMillan C, Moore P, Ding L, Glosser G, Work M, et al. What's in a name: voxel-based morphometric analyses of MRI and naming difficulty in Alzheimer's disease, frontotemporal dementia and corticobasal degeneration. Brain 2004; 127: 628–49.

Hayasaka S, Phan KL, Liberzon I, Worsley KJ, Nichols TE. Nonstationary cluster-size inference with random field and permutation methods. NeuroImage 2004; 22: 676–87.

Hickok G, Poeppel D. Dorsal and ventral streams: a framework for understanding aspects of the functional anatomy of language. Cognition 2004; 92: 67–99.

Hickok G, Poeppel D. The cortical organization of speech processing. Nat Rev Neurosci 2007; 8: 393–402.

Hodges JR, Patterson K. Nonfluent progressive aphasia and semantic dementia: a comparative neuropsychological study. J Int Neuropsychol Soc 1996; 2: 511–24.

Hodges JR, Patterson K, Oxbury S, Funnell E. Semantic dementia. Progressive fluent aphasia with temporal lobe atrophy. Brain 1992; 115 (Pt 6): 1783–806.

Kramer JH, Jurik J, Sha SJ, Rankin KP, Rosen HJ, Johnson JK, et al. Distinctive neuropsychological patterns in frontotemporal dementia, semantic dementia, and Alzheimer disease. Cogn Behav Neurol 2003; 16: 211–18.

Larsson EM, Englund E, Sjobeck M, Latt J, Brockstedt S. MRI with diffusion tensor imaging post-mortem at 3.0 T in a patient with frontotemporal dementia. Dement Geriatr Cogn Disord 2004; 17: 316–19.

Levine B, Stuss DT, Milberg WP, Alexander MP, Schwartz M, Macdonald R. The effects of focal and diffuse brain damage on strategy application: evidence from focal lesions, traumatic brain injury and normal aging. J Int Neuropsychol Soc 1998; 4: 247–64.

Lu LH, Crosson B, Nadeau SE, Heilman KM, Gonzalez-Rothi LJ, Raymer A, et al. Category-specific naming deficits for objects and actions: semantic attribute and grammatical role hypotheses. Neuropsychologia 2002; 40: 1608–21.

Makris N, Kennedy DN, McInerney S, Sorensen AG, Wang R, Caviness VS Jr, et al. Segmentation of subcomponents within the superior longitudinal fascicle in humans: a quantitative, in vivo, DT-MRI study. Cereb Cortex 2005; 15: 854–69.

Mandonnet E, Nouet A, Gatignol P, Capelle L, Duffau H. Does the left inferior longitudinal fasciculus play a role in language? A brain stimulation study. Brain 2007; 130: 623–9.

Matsuo K, Mizuno T, Yamada K, Akazawa K, Kasai T, Kondo M, et al. Cerebral white matter damage in frontotemporal dementia assessed by diffusion tensor tractography. Neuroradiology 2008; 50: 605–11.

McCulloch CE, Searle SR, Neuhaus JM. Generalized, linear, and mixed models. 2nd edn., New York: John Wiley and Sons; 2008.

Miller RG. edn. Simultaneous statistical inference. 2nd edn, New York: Springer-Verlag; 1981.

Mori S, Crain BJ, Chacko VP, van Zijl PC. Three-dimensional tracking of axonal projections in the brain by magnetic resonance imaging. Ann Neurol 1999; 45: 265–9.

Mummery CJ, Patterson K, Wise RJ, Vandenberghe R, Price CJ, Hodges JR. Disrupted temporal lobe connections in semantic dementia. Brain 1999; 122 (Pt 1): 61–73.

Mummery CJ, Patterson K, Price CJ, Ashburner J, Frackowiak RS, Hodges JR. A voxel-based morphometry study of semantic dementia: relationship between temporal lobe atrophy and semantic memory. Ann Neurol 2000; 47: 36–45.

Neary D, Snowden JS, Gustafson L, Passant U, Stuss D, Black S, et al. Frontotemporal lobar degeneration: a consensus on clinical diagnostic criteria. Neurology 1998; 51: 1546–54.

Patterson K, Hodges JR. Deterioration of word meaning: implications for reading. Neuropsychologia 1992; 30: 1025–40.

Perani D, Cappa SF, Schnur T, Tettamanti M, Collina S, Rosa MM, et al. The neural correlates of verb and noun processing. A PET study. Brain 1999; 122: 2337–44.

Petrides M, Pandya DN. Projections to the frontal cortex from the posterior parietal region in the rhesus monkey. J Comp Neurol 1984; 228: 105–16.

Rabinovici GD, Seeley WW, Kim EJ, Gorno-Tempini ML, Rascovsky K, Pagliaro TA, et al. Distinct MRI atrophy patterns in autopsy-proven Alzheimer's disease and frontotemporal lobar degeneration. Am J Alzheimers Dis Other Demen 2007; 22: 474–88.

Rosen HJ, Allison SC, Ogar JM, Amici S, Rose K, Dronkers N, et al. Behavioral features in semantic dementia vs other forms of progressive aphasias. Neurology 2006; 67: 1752–6.

Rosen HJ, Gorno-Tempini ML, Goldman WP, Perry RJ, Schuff N, Weiner M, et al. Patterns of brain atrophy in frontotemporal dementia and semantic dementia. Neurology 2002; 58: 198–208.

Rovaris M, Gass A, Bammer R, Hickman SJ, Ciccarelli O, Miller DH, et al. Diffusion MRI in multiple sclerosis. Neurology 2005; 65: 1526–32.

Schmahmann JD, Pandya DN, Wang R, Dai G, D'Arceuil HE, de Crespigny AJ, et al. Association fibre pathways of the brain: parallel observations from diffusion spectrum imaging and autoradiography. Brain 2007; 130: 630–53.

Seeley WW. Selective functional, regional, and neuronal vulnerability in frontotemporal dementia. Curr Opin Neurol 2008; 21: 701–7.

Selnes OA, Knopman DS, Niccum N, Rubens AB. The critical role of Wernicke's area in sentence repetition. Ann Neurol 1985; 17: 549–57.

Silani G, Frith U, Demonet JF, Fazio F, Perani D, Price C, et al. Brain abnormalities underlying altered activation in dyslexia: a voxel based morphometry study. Brain 2005; 128: 2453–61.

Smith SM. Fast robust automated brain extraction. Hum Brain Mapp 2002; 17: 143–55.

Snowden JS, Neary D, Mann DM, Goulding PJ, Testa HJ. Progressive language disorder due to lobar atrophy. Ann Neurol 1992; 31: 174–83.

Song SK, Sun SW, Ramsbottom MJ, Chang C, Russell J, Cross AH. Dysmyelination revealed through MRI as increased radial (but unchanged axial) diffusion of water. NeuroImage 2002; 17: 1429–36.

Sonty SP, Mesulam MM, Weintraub S, Johnson NA, Parrish TB, Gitelman DR. Altered effective connectivity within the language network in primary progressive aphasia. J Neurosci 2007; 27: 1334–45.

Sullivan EV, Rohlfing T, Pfefferbaum A. Quantitative fiber tracking of lateral and interhemispheric white matter systems in normal aging: relations to timed performance. Neurobiol Aging 2008 [Epub ahead of print].

Taoka T, Iwasaki S, Sakamoto M, Nakagawa H, Fukusumi A, Myochin K, et al. Diffusion anisotropy and diffusivity of white matter tracts within the temporal stem in Alzheimer disease: evaluation of the ''tract of interest'' by diffusion tensor tractography. AJNR Am J Neuroradiol 2006; 27: 1040–5.

Vernooij MW, de Groot M, van der Lugt A, Ikram MA, Krestin GP, Hofman A, et al. White matter atrophy and lesion formation explain the loss of structural integrity of white matter in aging. NeuroImage 2008; 43: 470–7.

Wakana S, Jiang H, Nagae-Poetscher LM, van Zijl PC, Mori S. Fiber tract-based atlas of human white matter anatomy. Radiology 2004; 230: 77–87.

Wilson SM, Brambati SM, Henry RG, Handwerker DA, Agosta F, Miller BL, et al. The neural basis of surface dyslexia in semantic dementia. Brain 2009; 132: 71–86.

Xie S, Xiao JX, Wang YH, Wu HK, Gong GL, Jiang XX. Evaluation of bilateral cingulum with tractography in patients with Alzheimer's disease. Neuroreport 2005; 16: 1275–8.

Yamauchi H, Fukuyama H, Nagahama Y, Katsumi Y, Hayashi T, Oyanagi C, et al. Comparison of the pattern of atrophy of the corpus callosum in frontotemporal dementia, progressive supranuclear palsy, and Alzheimer,s disease. J Neurol Neurosurg Psychiatry 2000; 69: 623–9.

Yasmin H, Nakata Y, Aoki S, Abe O, Sato N, Nemoto K, et al. Diffusion abnormalities of the uncinate fasciculus in Alzheimer's disease: diffusion tensor tract-specific analysis using a new method to measure the core of the tract. Neuroradiology 2008; 50: 293–9.

Zhang Y, Schuff N, Du AT, Rosen HJ, Kramer JH, Gorno-Tempini ML, et al. White matter damage in frontotemporal dementia and Alzheimer's disease measured by diffusion MRI. Brain 2009 [Epub ahead of print].